Clays and Clay Minerals, Vol. 64, No. 5, 552–559, 2016.

SYNTHETIC ZEOLITES DERIVED FROM FLY ASH AS EFFECTIVE MINERAL SORBENTS FOR DIESEL FUEL SPILL REMEDIATION

PINGQIANG GAO[1,2], YAN ZHANG[2], AND LIN ZHAO[1,*]

[1] School of Environment Science and Engineering, Tianjin University, 92 Weijin Road, Nankai District, Tianjin, 300072, P. R. China

[2] School of Chemistry and Chemical Engineering, Yulin University, 4 Chongwen Road, Yulin City, Shaanxi, 719000, P. R. China

Abstract—Development of an effective sorbent for diesel fuel spill remediation remains an important challenge in the field of synthesis due to the potential capacity of sorbents to efficiently purify contaminated sites. Fly ash, a coal combustion by-product, was used as a raw material to synthesize two inexpensive zeolites (SZ-1 and SZ-2) for oil spill remediation using an alkali fusion approach prior to hydrothermal treatment. The sorbents were characterized using scanning electron microscopy (SEM), transmission electron microscopy (TEM), X-ray diffraction (XRD), and N_2 adsorption/desorption. Diesel fuel sorption was used to examine the potential capacity of the synthetic zeolites to sorb oil and other petroleum products. Diesel fuel viscosity and density were determined at room temperature using a viscometer and a pycnometer, respectively. The synthetic zeolites exhibited a higher diesel fuel sorption capacity than fly ash. The SZ-1 zeolite sorbed approximately 1.43 $g \cdot g^{-1}$ and SZ-2 sorbed approximately 1.9 $g \cdot g^{-1}$. The sorption was mainly a physical process and mesopore filling seemed to play the dominant role. Sorbent textures were, therefore, vital for the sorption of petroleum products.

Key Words—Diesel Fuel, Esterification, Fly Ash, Hydrophobic Surface Functionalization, Mesopore, Oil Spill, Sorbents, Sorption, Stearic Acid, Surface Area, Zeolite.

INTRODUCTION

The sorption and removal of petroleum products is currently a growing worldwide concern due to the increasing risks of environmental pollution during petroleum recovery, transport, processing, storage, and exploitation (Wang *et al.*, 2012). Examples of diesel fuel spills in recent years include the loss of 24,000 barrels (1 million gallons) into the Monongahela River due to a ruptured storage tank in 1998, the large oil spill (approximately 20 million gallons) in the Galician coast of Spain in 2002 by the *Prestige* oil tanker, and the BP Deepwater Horizon spill (210 million gallons) in the Gulf of Mexico in 2010 that was caused by a wellhead blowout. In addition to financial losses, such incidents create an adverse impact on the Earth's ecosystems and a long-term harmful effect on living organisms (Zhang *et al.*, 2012; Leewis *et al.*, 2013; Franci *et al.*, 2014). These sources of environmental pollution seriously threaten the local environment. Hence, more efficient cleanup skills and more advanced materials are needed that can be applied to oil spill remediation.

Currently, three main methods are used to remove petroleum products, namely, mechanical, biological, and photochemical methods. Mechanical methods that involve solid absorbents have been considered the most effective. Absorbents can be grouped into three major classes: inorganic mineral products (*e.g.* zeolite, sorbent clay, and diatomite), synthetic organic products (*e.g.* polyurethane foam), and organic vegetable products (*e.g.* corn cobs and wood fiber) (Adebajo *et al.*, 2003).

Much research in recent years has focused on mineral materials for diesel fuel spill treatment. Mineral sorbents are non-flammable, cheap, and readily available. Additionally, mineral sorbents can keep the sorbed diesel fuel inside of a stable porous structure and the sorbed diesel fuel will not be released under higher pressure. Among mineral sorbents, zeolites are important and widely used due to the special properties (Pathak and Srivastava, 2012). Zeolites are clay materials and belong to the group of aluminosilicates that have open frameworks with different size and shape channels and pores (Fullen *et al.*, 2011). The regular system of channels and chambers creates several unique properties in both natural and synthetic zeolites, including sorption capacity, ion-exchange, molecular sieve, and catalytic properties. Synthetic zeolites, which are commonly produced from clay minerals (Pichor *et al.*, 2014), chemicals (Liu *et al.*, 2013), and fly ash (Wdowin *et al.*, 2014; Franus, 2012), exhibit better sorption properties than natural zeolites (Cardoso *et al.*, 2015). Among the feedstock materials, fly ash is a by-product obtained from the combustion of coal in thermoelectric power plants to generate electricity and is the cheapest. The use of zeolites synthesized from fly ash is particularly interesting in that it allows undesirable waste to be converted into a high value-added product.

* E-mail address of corresponding author:
zhaolin@tju.edu.cn
10.1346/CCMN.2016.064035

A hydrothermal process is the most common method to convert fly ash into zeolites; however, some studies have found that zeolites produced from fly ash have a low purity and a low sorption efficiency (Cardoso *et al.*, 2015). Alkali fusion has been a general method for decomposing materials containing Si and Al in chemical analysis (Wang *et al.*, 2007; Hillenbrand, 1962). Chang and Shilh (1998) converted fly ash to zeolite P by a significantly improved fusion method in which NaOH was fused with fly ash prior to conventional zeolite synthesis.

The aim of this paper was to measure the oil sorption capacity of two different types of synthetic zeolites, using diesel fuel as a representative adsorbate compound. The zeolites were synthesized from fly ash using the fusion approach prior to hydrothermal treatment.

MATERIALS AND METHODS

Materials

Fly ash was obtained from the Shangwan thermoelectric power plant in Yulin, Shaanxi, China. Hydrochloric acid (HCl) and toluene were obtained from Xilong Chemical Industry Co. (Sichuan, China). Sodium hydroxide (NaOH) and stearic acid ($C_{18}H_{36}O_2$) were purchased from Kemiou Chemical Reagent Co. (Tianjin, China). All other chemicals were of analytical grade and were used as received without further purification.

Diesel fuel was obtained from Shaanxi Yanchang Petroleum Co., LTD (Yulin, Shaanxi, China). The kinematic viscosity of the diesel fuel was 2.1 cSt (mm^2/s), as measured using a DNJ-8S viscometer (Fang Rui Instrument Co., Shanghai, China) at room temperature. The density was 0.812 $g{\cdot}cm^{-3}$, as measured using a pycnometer.

Methods

Raw fly ash was converted to zeolite by the methods of Mainganye *et al.* (2013) and Ramirez *et al.* (2014). In this process, 1 g of fly ash was first reacted with 10 mL 20% HCl at 80ºC for 2 h, then dried at 105ºC. The acid-treated fly ash was then mixed with NaOH powder (fly ash/NaOH = 1/1.25 ratio by weight) and heated in air at 550ºC for 2 h at a heating rate of 5ºC/min. After fusion, the powder was ground and 10 g was dispersed in 50 mL of distilled water, followed by aging with stirring for 24 h at room temperature and ambient pressure. The resulting slurry was crystallized at 120ºC for 12 h. After synthesis, the solid products formed were recovered by filtration and washed with deionized water. The product was then dried in a vacuum oven at 105ºC, 0.1 MPa, and labeled SZ-1. The synthetic procedure for SZ-2 was the same as for SZ-1, except the crystallization temperature for SZ-2 was 90ºC instead of 120ºC.

The two zeolite types (SZ-1 and SZ-2) were treated using an esterification reaction for hydrophobic surface functionalization. Stearic acid (5.7 g) was accurately weighed and dissolved in 60 mL of a NaOH solution (3 mol/L) at 80ºC. Next, 5 g of sample was added and the slurry was stirred until the system slowly cooled to room temperature, which allowed the stearic acid to precipitate and coat the sample particles. The coated particles were filtered and washed several times with water to remove NaOH until filtrate pH was 7. The powder was then dried and placed in a furnace at 180ºC for 4 h to induce chemical bonding of the stearic acid carboxyl groups to the sample surface. The samples were washed several times with hot toluene and water to remove excess stearic acid. Sufficient washing to remove excess stearic acid was indicated by disappearance of the waxy solid. The washed samples were oven-dried at 100ºC to a constant weight.

Material characterization

A FEI Nanosem 430 (FEI, Hillsboro, Oregon, USA) scanning electron microscope (SEM) was used to observe the morphology of the sample particles, after vacuum coating with a gold film. Energy-dispersive X-ray (EDS) analysis combined with SEM using EDAX software were applied at 15.0 kV and 20.0 μA to perform elemental analyses of the samples. Zeolite samples were ultrasonically treated to break up large aggregates,

Table 1. Physicochemical properties of raw fly ash, SZ-1 and SZ-2.

Parameter	Atom %		
	[a]Fly ash	SZ-1 (Na-P1)	SZ-2 (Faujasite)
O	40.81±0.77	54.18±0.64	55.12±0.52
Al	22.87±0.23	15.11±0.21	15.56±0.13
Si	32.32±0.18	20.70±0.26	17.63±0.16
Na		6.81±0.23	8.48±0.25
Fe	3.21±0.22	3.20	3.21
Mg	0.61±0.07		
Ti	0.07±0.04		
Ca	1.11±0.12		

[a] The instrument counting error (±) in elemental content.

https://doi.org/10.1346/CCMN.2016.064035 Published online by Cambridge University Press

Table 2. Textural parameters for fly ash, SZ-1, and SZ-2.

Sorbent	S_{BET} (m^2/g)	S_{mic}t-plot (m^2/g)	S_{ext}t-plot m^2/g)	V_{tot} (cm^3/g)	V_{mic}t-plot (cm^3/g)	D_p (nm)
Fly ash	25.61	0.021	18.84	0.079	0.0001	13.13
SZ-1(Na-P1)	169.74	12.21	109.52	0.61	0.0043	21.34
SZ-2(Faujasite)	246.07	6.86	170.42	0.79	0.0014	18.39

S_{BET} – specific surface area; S_{mic} – micropore area; S_{ext} – external surface area; V_{tot} – pore volume; D_p – average pore diameter; V_{mic} – micropore volume.

coated with vacuum-evaporated gold, and a Philips CM 120 (Philips, Amsterdam, The Netherlands) transmission electron microscope was used to examine the samples and determine particle size. Powder X-ray diffraction (XRD) of the samples was performed using a Bruker X-ray diffractometer (Bruker company, Karlsruhe, Germany) with a CuKα radiation source (λ = 0.15406 nm) and were scanned from 5º to 60º2θ. BET surface area was determined by nitrogen adsorption/desorption at −194.85ºC using a Micromeritics ASAP 2020 device (Micromeritics Instruments, Norcross, Georgia, USA) and liquid N_2. Samples were first outgassed at 120ºC for 4 h and then further outgassed at 180ºC for 6 h. The BET specific surface area, BJH (Barret-Joyner-Halenda) nanopore size distribution functions, total pore volume, micropore volume, and external surface area based on the *t*-plot method were then calculated using ASAP 2020 software provided by the equipment manufacturer.

Oil sorption capacity measurements were conducted at room temperature according to the procedure of Tamilselvan *et al.* (2013) using diesel fuel to represent the oil. Five grams of the zeolite samples were mixed with different amounts of diesel fuel in a beaker and stirred for 24 h, followed by vacuum filtration using a Buchner funnel. With the vacuum pump running, the samples were scraped from the filter paper after 10 min of filtration and placed in a vial for thermogravimetric analysis (TGA). The diesel fuel to sorbent weight ratio (w/w) ranged from 0.25 to 2.0.

TGA analyses were conducted using a Mettler TGA/DSC1 (Mettler Instruments, Toledo, Ohio, USA) with a heating rate of 20ºC min^{-1} under a 100 mL min^{-1} air flow. For each specimen, TGA was also conducted on the powder sample prior to diesel fuel sorption. The diesel fuel sorption capacity was calculated from the difference in the wt.% lost between 100ºC and 500ºC for each sample before and after diesel fuel sorption.

RESULTS AND DISCUSSION

Physiochemical properties of raw fly ash

Fly ash is a fine, gray powder and EDS analysis (Table 1) revealed that the major constituents are SiO_2, Al_2O_3, CaO, and Fe_2O_3. The fly ash particles consist largely of solid or hollow spherical particles of variable size with small bulging regions of siliceous and aluminous glass with cracks at the top of the bulges (Figures 1a, 1b). The photomicrographs indicated that the gray sheets were mixtures of coal and ash. The BET surface area was 25.61 $m^2 \cdot g^{-1}$ (Table 2). The EDS analysis confirmed that the matrix around the porous areas had an aluminosilicate composition with a Si-to-Al atomic ratio of 1.41 and an O-to-total weight ratio of 0.40. The Ca content was 1.11%, which is consistent with the class F designation (ASTM C618-15), whereas the Fe content was low (3.5%, Table 1).

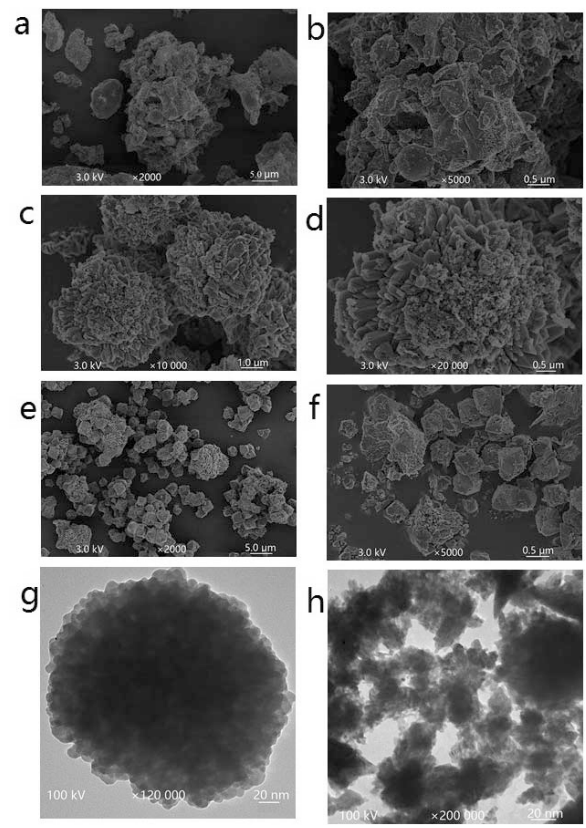

Figure 1. Fly ash and synthetic zeolite electron microscopy: (a, b) SEM images of fly ash, (c, d) SEM images of SZ-1, (e, f) SEM images of SZ-2 at different magnifications, (g) TEM image of SZ-1, and (h) TEM image of SZ-2.

https://doi.org/10.1346/CCMN.2016.064035 Published online by Cambridge University Press

Mineralogical characteristics

The XRD patterns of raw fly ash (Figure 2a) showed that the major crystalline phases were quartz (SiO_2) and mullite ($3Al_2O_3{\cdot}2SiO_2$), with a small amount of lime (CaO). This XRD result is consistent with the SEM images (Figure 1b).

All peaks in the XRD pattern of SZ-1 (Figure 2b) matched the structure of a P-type zeolite according to Cardoso *et al*. (2015). The XRD pattern showed that the crystalline phases of quartz and mullite in the raw fly ash were absent in the zeolite material after the synthesis reaction and that Na^+ was the main cation balancing the charge of the aluminosilicate. The EDS analysis of SZ-1 (Table 1) indicated the Si/Al ratio was reduced from 1.41 to 1.37 and showed that the higher alkali solution concentration dissolved Si and Al species from the fly ash, and consequently decreased the Si/Al ratio. Aluminosilicates dissolve in the alkali solutions due to the formation of Na silicates and possibly amorphous aluminosilicates.

The conversion of fly ash into a second zeolite phase (SZ-2) by lowering the crystallization temperature: this phase was identified as faujasite as confirmed by XRD analysis (Figure 1c; Chang and Shih, 1998). The elemental composition of SZ-2 is given in Table 1. Similar to SZ-1, the Si/Al ratio of SZ-2 decreased to 1.11, but the Na content increased in comparison to SZ-1. This may relate to the crystallization temperature during hydrothermal treatment.

Microstructural analysis of SZ-1 and SZ-2 was achieved using SEM. Representative images of the different structures are shown in Figures 1c, 1d, 1e, and 1f. Images from sample SZ-1 (Figures 1c and 1d) revealed structures that are typical of zeolite Na-P1, as previously reported in the literature (Cardoso *et al.*, 2015; Ferret, 2004). The Na-P1 zeolite has pillars that form a range of rosette sizes that are typically 5 μm. The SEM images also confirmed that the zeolite particles in sample SZ-1 had stacked pores with rough grainy surfaces (Figure 1d).

The sample of SZ-2 showed aggregates consisting of particles with octahedral structure (Figure 1e), which is similar to the microstructure observed previously by Chang and Shih (1998). The particles composed of aggregates had a diameter of approximately 4 μm. A

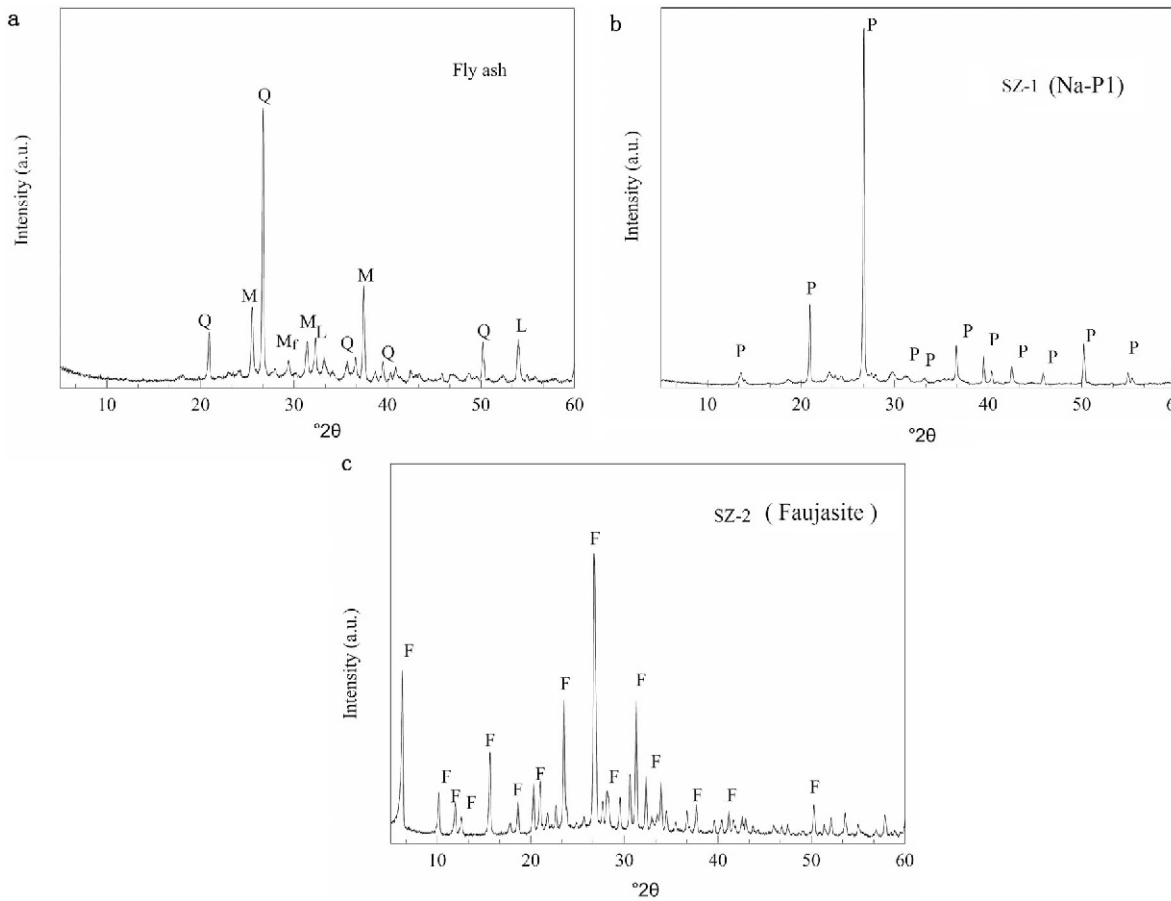

Figure 2. XRD patterns and identified mineral phases in (a) fly ash, (b) SZ-1, and (c) SZ-2. Q = quartz, M = mullite, L = lime, Mf = magnesio ferrite, P = zeolite Na-P1, and F = faujasite.

https://doi.org/10.1346/CCMN.2016.064035 Published online by Cambridge University Press

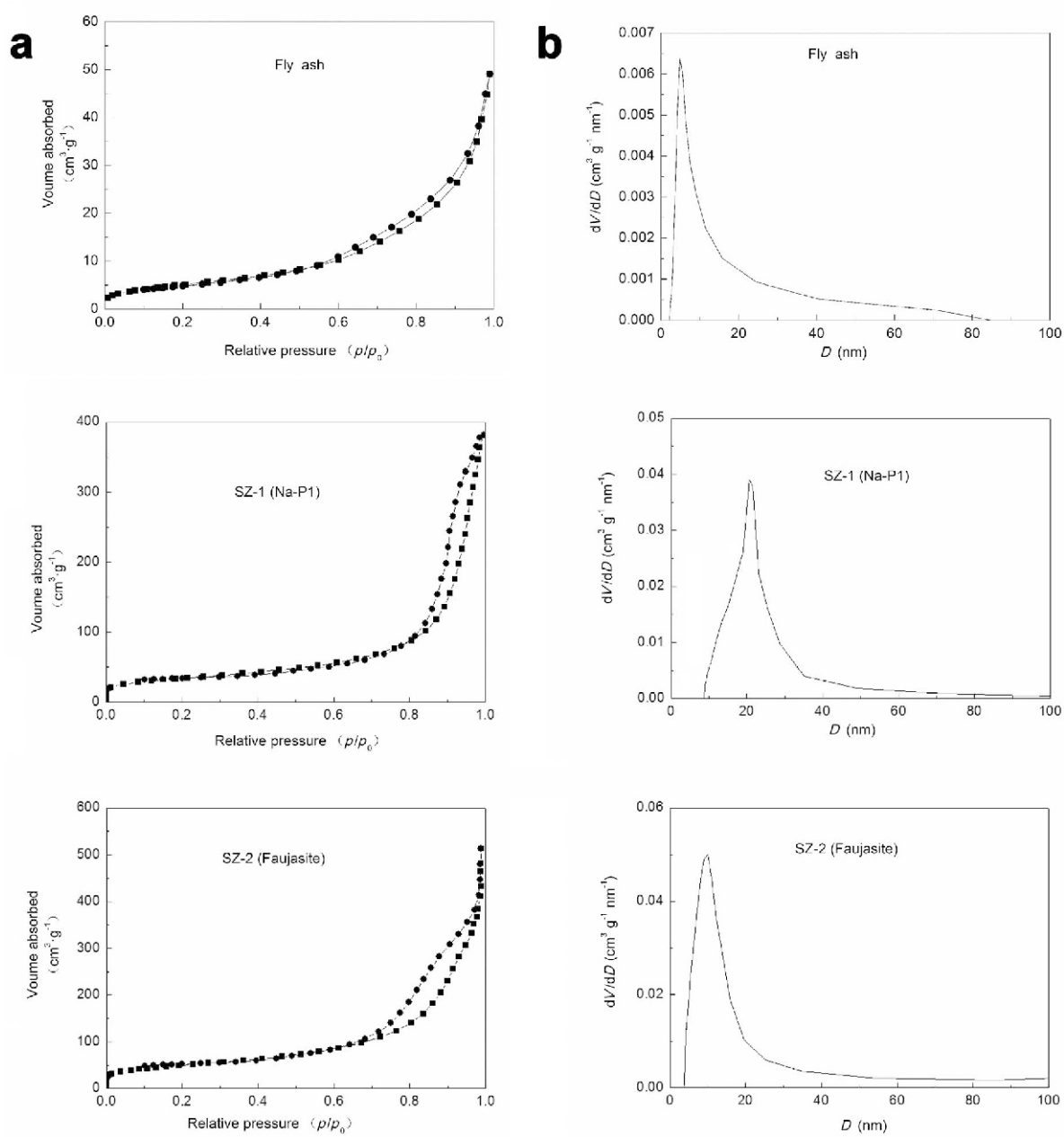

Figure 3. (a) The N_2 adsorption-desorption isotherms at 77 K and (b) BJH desorption pore size distributions of fly ash, SZ-1, and SZ-2.

porous structure was also observed (Figure 1f). The SEM images of these two types of synthetic zeolite show an absence of spherical particles, which indicates that complete dissolution and conversion of fly ash to form highly crystalline zeolites occurred during the treatment.

In order to investigate the porous structure of the samples, TEM micrographs of the samples were made. The TEM micrograph of SZ-1 (Figure 1g) shows that the sample consists of polycrystalline aggregates and has a uniform pore size distribution with pore diameters of about 20 nm. Zeolite SZ-2 (Figure 1h) formed crystals with uniform pores with a diameter of around 10 nm.

Nitrogen adsorption analysis

The nitrogen adsorption-desorption isotherms at −194.85ºC and the nanopore size distribution curves are presented in Figure 3. The adsorption branches of the isotherms with hysteresis loops belong to the type IV IUPAC classification (Sing, 2009), which indicates that the initial region of the isotherm can be attributed to monolayer-multilayer physical adsorption. This is because the initial isotherm region followed the same path as a corresponding region of a Type II isotherm obtained by adsorption to the same surface area of a non-porous form of the sorbent (Bandura *et al.*, 2015). Many mesoporous

https://doi.org/10.1346/CCMN.2016.064035 Published online by Cambridge University Press

sorbents yield type IV isotherms. Generally, the adsorption process over a range of general relative pressures (p/p_o near 0.5) is dominated by monomolecular adsorption. The next most dominant processes are multilayer and capillary condensation. An extremely rapid increase in nitrogen adsorption was observed for SZ-1 and SZ-2 at very low relative pressures (below 0.01). This result indicated strong adsorption at very low fractional pressures, which is characteristic of the micropores in faujasite.

The adsorption-desorption hysteresis loops were observed in the p/p_0 range of 0.50 to 0.93 for all materials, which indicates the existence of nano-sized pores (Kubů *et al.*, 2014; Sprynskyy *et al.*, 2005). Adsorption/desorption hysteresis loops were of the H3 type according to the IUPAC classification and were characterized as solids with slit-shaped pores. This conclusion is consistent with the sample SEM measurements.

The nanopore size distributions determined from the sample isotherms were homogenous. Pores of approximately 5.31, 17.21, and 12.21 nm were observed in fly ash, SZ-1, and SZ-2, respectively.

The textural parameters of fly ash, SZ-1, and SZ-2 (Table 2) showed that the BET specific surface area of SZ-2 was the highest, and the surface area was lowest for the fly ash. Fly ash had the narrowest pores, whereas the widest pores were observed in SZ-1. The SZ-2 had slightly smaller size pores than SZ-1. The largest total pore volume was in sample SZ-2 and the lowest in fly ash. The SZ-2 and SZ-1 had significantly larger pore volumes than fly ash.

Diesel fuel sorption

To investigate the maximum sorption capacity for diesel fuel by the analyzed samples, an adsorption test was performed with all three samples using pure diesel fuel without any water. After 24 h (Figure 4), at low diesel fuel to sample ratios, nearly all of the diesel fuel was sorbed. With increasing ratios, the sample pores became saturated and, eventually, an excess layer of diesel fuel was observed. This occurred when the diesel fuel to sample ratios reached 0.5 for fly ash, 1.0 for SZ-1, and 1.5 for SZ-2 (Figures 4a, 4b, and 4c).

The experimentally measured amounts of diesel fuel sorbed by the samples at different ratios (Figure 5) revealed that for ratios >1, the diesel fuel adsorption reached a constant level for SZ-1 and SZ-2 equal to the maximum sorption capacity. The maximum diesel fuel sorption capacity of fly ash (<0.2 $g \cdot g^{-1}$) was reached at a diesel fuel to sorbent ratio of 0.5. The SZ-2 sample had the largest sorption capacity (1.9 $g \cdot g^{-1}$), which indicated that this kind of synthetic zeolite (faujasite) was the most effective diesel sorbent. The sorption capacity of SZ-1 was slightly smaller (1.43 $g \cdot g^{-1}$) and the sorption capacity of fly ash was the smallest (approximately 0.18 $g \cdot g^{-1}$). Tamilselvan *et al.* (2013) prepared a zeolite material using fly ash as feedstock by alkali fusion and hydrothermal treatment and the diesel fuel sorption capacity of the zeolite prepared from fly ash was 1.15 $g \cdot g^{-1}$ in diesel fuel medium.

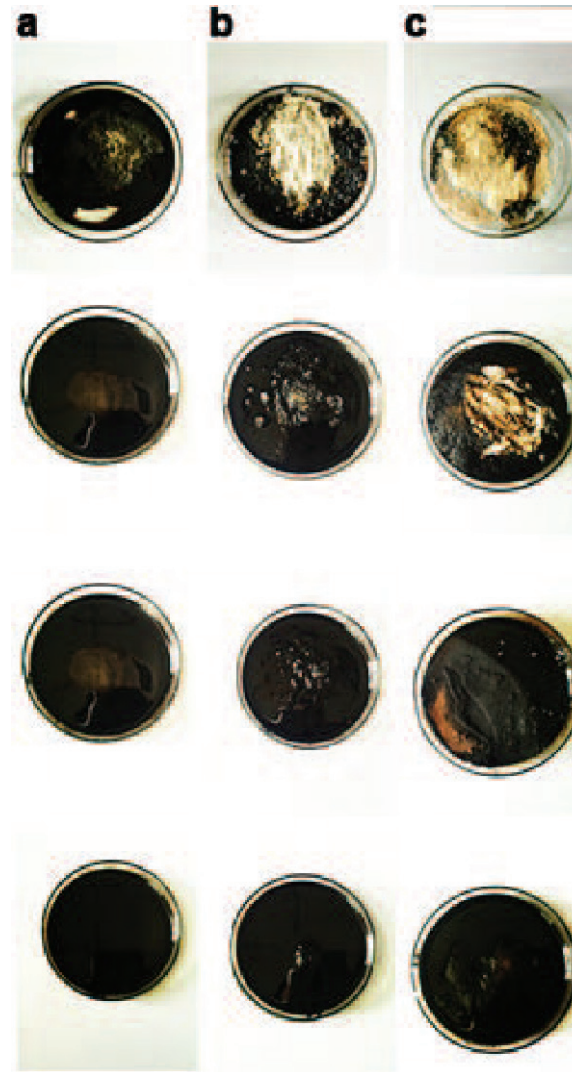

Figure 4. Sorption of diesel fuel by (a) fly ash, (b) SZ-1 (Na-P1), and (c) SZ-2 (faujasite) at diesel fuel/sorbent ratios, from top to bottom, of 0.50, 0.75, 1.00, and 1.50.

The sorbent material textural parameters seemed to govern the sorption capacity for petroleum products as postulated by Carmody *et al.* (2007). The average sample sorption capacity was (abbreviated SC) increased linearly with specific surface area ($SC = 0.0079S_{BET} + 0.00817$; $R^2 = 0.99$). The SC increased linearly with the sample mesopore volume, V_{es}, estimated as the total pore volume minus the micropore volume ($SC = 2.40029V_{es} - 0.01245$; $R^2 = 0.99$). The SC also increased linearly with the mesopore surface area ($SC = 0.01152S_{ext} + 0.02386$; $R^2 = 0.96$). The micropore volumes did not correlate with SC, which was possibly due to the very small volume. As a result, a higher surface area with a larger pore volume allowed more

https://doi.org/10.1346/CCMN.2016.064035 Published online by Cambridge University Press

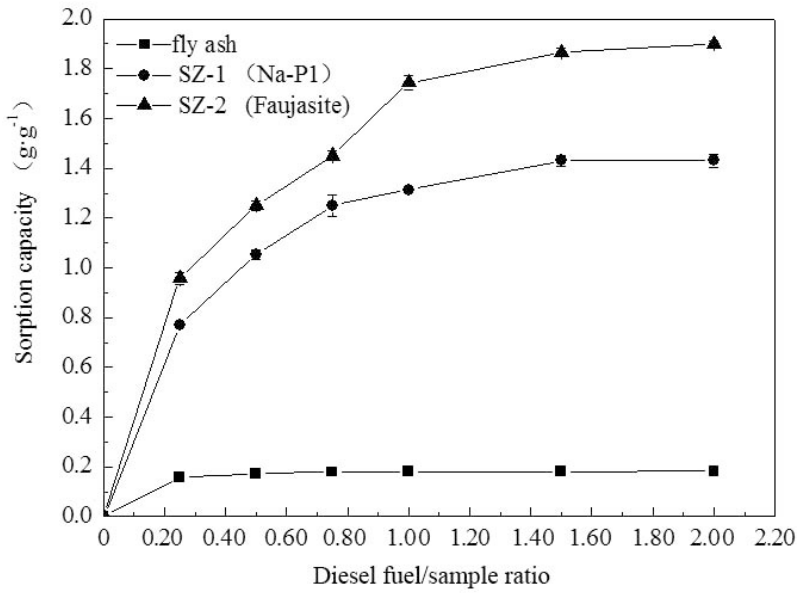

Figure 5. Diesel fuel sorption capacities of (a) fly ash, (b) SZ-1 zeolite, and (c) SZ-2 zeolite at different diesel fuel: zeolite sample ratios, from left to right, of 0.50, 0.75, 1.00, 1.50, and 2.00.

diesel fuel contact area on SZ-2 and allowed SZ-2 to sorb easily the highest amount of diesel fuel. Synthetic zeolites with larger surface areas and meso pre-pores (meso pre-pore = mesopore at initial stage of formation) can be beneficial for large hydrocarbon molecule access. That is why SZ-2 exhibited a higher diesel fuel capacity, despite having slightly smaller pore diameters. The analysis results indicate that petroleum product sorption on the synthetic zeolites was dominated by physical characteristics and that mesopore filling seemed to play the most important role.

CONCLUSIONS

The results demonstrated that the fly ash by-product obtained from coal combustion in thermoelectric power plants can be used as a raw material in the synthesis of the zeolites SZ-1 and SZ-2. Diesel fuel sorption by zeolite SZ-1 and SZ-2 was mainly a physical process and included mesopore filling and external surface coverage. Consequently, zeolite texture played an important role in petroleum product sorption capacity. Pore surfaces and BET surface areas were strongly correlated with diesel fuel sorption capacity. Zeolite SZ-1 had a seven-fold higher diesel fuel sorption capacity than the fly ash, whereas SZ-2 had a 10-fold higher diesel fuel sorption capacity than the fly ash.

Synthetic zeolites derived from fly ash are an interesting alternative to widely used sorbents for diesel fuel spill cleanup due to the unique diesel fuel sorption capacity. In addition, the application of zeolites synthesized from waste fly ash is a good example of a sustainable and ecologically beneficial method for environmental protection.

ACKNOWLEDGMENTS

The authors acknowledge the National Science Foundation for Young Scientist of China (Grant No. 51502261) and the project from Tianjing Oceanic Administration (Grant No.201455-0001) to make this study possible.

REFERENCES

Adebajo, M.O., Frost, R.L., Kloprogge, J.T., Carmody, O., and Kokot, S. (2003) Porous materials for diesel fuel spill cleanup: a review of synthesis and absorbing properties. *Journal of Porous Materials*, **10**, 159–170.

ASTM C618-15, Standard specification for coal fly ash and raw or calcined natural pozzolan for use in concrete, ASTM International, West Conshohocken, PA, 2015, www.astm.org.

Bandura, L., Franus, M., Józefaciuk, G., and Franus, W. (2015) Synthetic zeolites from fly ash as effective mineral sorbents for land-based petroleum spills cleanup. *Fuel*, **147**, 100–107.

Cardoso, A.M., Paprocki, A., Ferret, L.S., Azevedo, C.M.N., and Pires, M. (2015) Synthesis of zeolite Na-P1 under mild conditions using Brazilian coal fly ash and its application in wastewater treatment. *Fuel*, **139**, 59–67.

Carmody, O., Frost, R., Xi, Y., and Kokot, S. (2007) Surface characterization of selected sorbent materials for common hydrocarbon fuels. *Surface Science*, **601**, 2066–2076.

Chang, H.L. and Shih, W.H. (1998) A general method for the conversion of fly ash into zeolites as ion exchangers for cesium. *Industrial & Engineering Chemistry Research*, **37**, 71–78.

Ferret, L.S. (2004) Zeolite from coal ash: synthesis and use. PhD thesis, Metallurgical and Materials-PPGEM, Federal University of Rio Grande do Sul, Av. Paulo Gama, Porto Alegre, Rio Grande do Sul, Brazil, 139 pp.

Franci, C.D., Guillemette, M., Pelletier, E., Chastel, O., Bonnefoi, S., and Verreault, J. (2014) Endocrine status of a migratory bird potentially exposed to the deepwater horizon diesel fuel spill: a case study of northern gannets breeding on Bonaventure Island, eastern Canada. *Science of*

https://doi.org/10.1346/CCMN.2016.064035 Published online by Cambridge University Press

the Total Environment, **473-474**, 110–116.

Franus, W. (2012) Characterization of X-type zeolite prepared from coal fly ash. *Polish Journal of Environmental Studies*, **21**, 337–343.

Fullen, M.A., Kelay, A., and Williams, C.D. (2011) Remediation of diesel fuel spills using zeolites. The 6th International Congress of European Society for Sdiesel fuel Conservation "Innovative Strategies and Policies for Sdiesel fuel Conservation," 120 in Thessaloniki, Greece.

Hillenbrand, W.F., Lundell, G.E.F., Bright, H.A., and Hoffman, J.I. (1962) *Applied Inorganic Analysis, 2nd e*d.; Wiley, New York.

Kubů, M., Opanasenko, M., and Shamzy, M. (2014) Modification of textural and acidic properties of -SVR zeolite by desilication. *Catalysis Today*, **227**, 26–32.

Leewis, M.-C., Reynolds, C.M., and Leigh, M.B. (2013) Long-term effects of nutrient addition and phytoremediation on diesel and crude diesel fuel contaminated sdiesel fuels in subarctic Alaska. *Cold Regions Science and Technology*, **96**, 129–137.

Liu, M., Hou, L., and Xi, B. (2013) Synthesis, characterization, and mercury adsorption properties of hybrid mesoporous aluminosilicate sieve prepared with fly ash. *Applied Surface Science*, **273**, 706–716.

Mainganye, D., Ojumu, T.V., and Petrik, L. (2013) Synthesis of zeolites Na-P1 from South African coal fly ash: Effect of impeller design and agitation. *Materials*, **6**, 2074–2089.

Pathak, C. and Srivastava, V.K. (2012) Silica reduction technology for fly ash zeolite synthesis. *International Journal of Pure & Applied Sciences & Technology*, **9**, 47–51.

Pichor, W., Mozgawa, W., and Krol, M. (2014) Synthesis of the zeolites on the lightweight aluminosilicate fillers. *Materials Research Bulletin*, 2014, **49**, 210–215.

Ramírez, A.M., Melo, P.G., and Robles, J.M.A. (2014) Synthesis of nanoporous materials and their functionalization for environmental applications. *Materials Science Forum*, **783–786**, 2005–2010.

Sing, K.S.W. (2009) Reporting physisorption data for gas/solid systems with special reference to the determination of surface area and porosity. *Pure & Applied Chemistry*, **54**, 2201–2218.

Sprynskyy, M., Lebedynets, M., Terzyk, A.P., Namieśnik, J., and Buszewski, B. (2005) Ammonium sorption from aqueous solutions by the natural zeolite Transcarpathian clinoptilolite studied under dynamic conditions. *Journal of Colloid & Interface Science*, **284**, 408–415.

Sakthivel, T., Reid, D. L., Goldstein, I., Hench, L., and Seal, S. (2013) Hydrophobic high surface area zeolites derived from fly ash for diesel fuel spill remediation. *Environmental Science & Technology*, **47**, 5843–5850.

Wang, J., Zheng, Y., and Wang, A. (2012) Effect of kapok fiber treated with various solvents on diesel fuel absorbency. *Industrial Crops and Products*, **40**, 178–184.

Wang, S.B., Li, L., and Zhu, Z.H. (2007) Solid-state conversion of fly ash to effective adsorbents for Cu removal from wastewater. *Journal of Hazardous Materials B*, **139**, 254–259.

Wdowin, M., Franus, M., and Panek, R. (2014) The conversion technology of fly ash into zeolites. *Clean Technologies and Environmental Policy*, **16**, 1217–1223.

Zhang, J., Dai, J., Chen, H., Du, X., Wang, W., and Wang, R. (2012) Petroleum contamination in ground water/air and its effects on farmland sdiesel fuel in the outskirt of an industrial city in China. *Journal of Geochemical Exploration*, **118**, 19–29.

(*Received 7 May 2016; revised 14 September 2016; Ms. 1107; AE: S.M. Kuznicki*)